1-1-2017

Microgrid Control Strategy Study and Controller Design Based on Model Predictive Control

Yitong Shen
University of Denver

MICROGRID CONTROL STRATEGY STUDY AND CONTROLLER DESIGN BASED ON MODEL PREDICTIVE CONTROL

A Thesis

Presented to

the Faculty of the Daniel Felix Ritchie School of Engineering and Computer Science

University of Denver

In Partial Fulfillment

of the Requirements for the Degree

Master of Science

by

Yitong Shen

March 2017

Advisor: Dr. David Wenzhong Gao

Author: Yitong Shen
Title: MICROGRID CONTROL STRATEGY STUDY AND CONTROLLER DESIGN BASED ON MODEL PREDICTIVE CONTROL
Advisor: Dr. David Wenzhong Gao
Degree Date: March 2017

ABSTRACT

In the 21st century, because of the exhausting of oil, coal and other non-renewable energy, human beings enter a period of large-scale exploitation and utilization of renewable energy. Renewable energy generation becomes an important way for new energy usage, however, as more and more distributed generation connect to power distribution network, the traditional distribution network structure will be changed. A large number of distributed generation applications of modern power electronic technology have also produced a lot of harmonics to impact the power quality. It will threaten the safe operation of the distribution network and obstruct the utilization of renewable energy. The concept of microgrid provides a new thinking for the application of renewable energy. A microgrid can make full use of the characteristics of the renewable energy, and it is the key to the future resources and environment for human beings. We can predict that microgrid construction will be rapidly developed in the 21st century, based on the utilization of renewable energy.

To coordinate the contradiction between the power grid and distributed generation, the concept of microgrid arises at the historic moment. Microgrid has two operation modes:

islanded mode and grid-connected mode. By theoretically analyzing, simulation model construction and result investigating, the microgrid coordinated control strategies will be studied in this paper.

Firstly, this paper starts from the microgrid operation control mode, respectively establishing the traditional control strategy of simulation for the isolated and grid-connected microgrid. The isolated grid control strategy is droop control strategy based on droop characteristic, and the grid-connected control strategy is P/Q control strategy.

Second, in chapter three, the principle and application of model predictive control are introduced. In the case study, the traditional PI controller is compared with model predictive control controller in single distributed generation system to present advantages of the model predictive control method.

Last, the model of a microgrid with multiple distributed generations is built in MATLAB/Simulink. There are three cases in this model: working model switches between grid-connected and islanded mode; increase and decrease load in islanded mode; disconnect one PV system at a certain time in islanded mode. By analyzing results of three cases, the MPC controller can achieve desirable efficiency of power control. Meanwhile, the voltage and frequency are working in the required range of the system. That proves the effectiveness of MPC controller.

ACKNOWLEDGMENTS

First of all, I would like to extend my sincere gratitude to my advisor Prof. David Wenzhong Gao, for his instructive advice and useful suggestions on my thesis and his selfless support during my two years study at the University of Denver.

I am also grateful to the committee chair Prof. Andrew Detzel and committee members, Prof. Jason Jun Zhang, and Prof. Amin Khodaei. Thank you for your time in checking the thesis draft and giving your valuable suggestions.

Special thanks should go to my lab mates in Renewable Energy and Power Electronics Lab at the University of Denver. I appreciate your help when I meet difficulties.

Finally, I am indebted to my parents for their continuous support and encouragement.

TABLE OF CONTENTS

CHAPTER ONE: INTRODUCTION 1
1.1 Background and Motivation 1
1.2 Microgrid Control Techniques 2
1.3 Literature Review 5
1.4 Expected Contribution 9

CHAPTER TWO: MICROGRID CONTROL STRATEGY STUDY 10
2.1 The Inverter of Grid-connected Microgrid Controller 10
2.2 The LC filter 13
2.3 Microgrid Control Strategy 13
2.3.1 The Active and Reactive Power Decoupling 14
2.3.2 PQ controller 15
2.3.3 Droop control 16

CHAPTER THREE: MODEL PREDICTIVE CONTROL 22
3.1 Principle of Model Predictive Control (MPC) 22
3.2 MPC Controller 24
3.2.1 PQ controller with MPC 24
3.2.2 Droop controller with MPC 27
3.3 The MPC Controller Model Simulation 28
3.3.1 PQ MPC controller simulation 28
3.3.2 Droop MPC controller simulation 29
3.3.3 Simulation result 30

CHAPTER FOUR: CASE STUDY 34
4.1 The Microgrid Model and Parameters 34
4.2 Microgrid Model Simulation 36
4.2.1 Working model switches between grid-connected and islanded mode 36
4.2.2 Increase and decrease load in islanded mode 39
4.2.3 Disconnect one PV system at certain time in islanded model. 41
4.3 Discussion 43

CHAPTER FIVE: CONCLUSION AND FUTURE WORK 45
5.1 Conclusion 45
5.2 Future Work 45

REFERENCE 46

LIST OF TABLES

Table 3.1 The parameters of PQ controller.....29
Table 3.2 The parameter of droop controller.....32

Table 4.1 PV source parameters 35
Table 4.2 Microgrid parameters.....35
Table 4.3 Load parameters.....35

LIST OF FIGURES

Figure 1.1 The master-slave control structure 3
Figure 1.2 The peer to peer control structure 3

Figure 2.1 Topologic structure of inverter in three-phase grid 10
Figure 2.2 PQ controller diagram 15
Figure 2.3 Power transmission vector diagram 16
Figure 2.4 P/f droop curve 18
Figure 2.5 Q/U droop curve 18
Figure 2.6 Droop controller diagram 19
Figure 2.7 Power controller diagram 20
Figure 2.8 Diagram of voltage current double loop 20

Figure 3.1 Principle of model predictive control 23
Figure 3.2 PQ controller based on MPC 25
Figure 3.3 MPC controller flow chart 26
Figure 3.4 Droop controller based on MPC 27
Figure 3.5 Diagram of one source with MPC controller in grid-connected mode 27
Figure 3.6 Diagram of one source with MPC controller in islanded mode 28
Figure 3.7 the active power of inverter output with two controllers in case 1 30
Figure 3.8 the reactive power of inverter output with two controllers in case 1 30
Figure 3.9 the reactive power of inverter output with two controllers in case 2 31
Figure 3.10 the active power of inverter output with two controllers in case 2 31
Figure 3.11The frequency response in case 3 33

Figure 4.1 Microgrid Diagram 34
Figure 4.2.1.1 Active power of three PV 37
Figure 4.2.1.2 Reactive power of three PV 37
Figure 4.2.1.3 Bus voltage 37
Figure 4.2.1.4 System frequency 38
Figure 4.2.2.1 Active power of three PV 39
Figure 4.2.2.2 Reactive power of three PV 39
Figure 4.2.2.3 Bus voltage 40
Figure 4.2.2.4 System frequency 40
Figure 4.2.3.1 Active power of three PV 41
Figure 4.2.3.2 Bus voltage 41
Figure 4.2.3.3 System frequency 42

CHAPTER ONE: INTRODUCTION

1.1 Background and Motivation

The utility grid in the decade became the main power supply mode in the world with the growing demand for electricity. However, it is gradually revealed some problems, such as the difficulty running and the high cost, and it is also difficult to meet the safety and reliability requirement in load with the increasingly high demand.

The Northeast Blackout of 2003 fully exposed the vulnerabilities and other issues of the utility grid. Therefore, the microgrid is officially studied by our researcher.

Before the 2003 Northeast Blackout, the concept of a microgrid is proposed on the white paper of Consortium for Electric Reliability Technology Solutions(CERTS) in 2002[1]. Microgrid, which is composed by the load, distributed generation(DG) and energy storage, can provide the electricity and heat at the same time; the power electronic devices convert the power supply of microgrid and provides the necessary control to microgrid[2]. By using varies of renewable energy, the microgrid can provide the uninterrupted power supply, enhance the stability of local electricity grid and compensate voltage to the local grid.

Microgrid has some advantage:

(1) Because the distributed generation is closed to the local loads, the microgrid can save lot of money in long distance transmission and decrease the loss in transmission to improve the power efficiency;

(2) A microgrid can work in two modes: grid-connected and islanded mode. The microgrid usually works in the grid- connected mode. However, when the blackout happens in the utility grid, the microgrid can operate in islanded mode to make sure that the load can be served with standard power supply.

(3) Through the microgrid control, we can avoid the mutual influence which is caused by the voltage and frequency fluctuations between regions, to prevent the blackout due to the partial grid malfunction.

Microgrid control is a crucial objective for research. How to control the active and reactive power, the output voltage, and frequency of microgrid and make it working steady, efficiently and economically, is very significant.

1.2 Microgrid Control Techniques

Nowadays, there are three primary control structures in microgrid control: master-slave control, peer to peer control and hierarchic control [3].

In the master-slave control structure, when microgrid working in islanded mode, the voltage and frequency in one of the DG or energy storage are used as the reference

value to other DGs and loads. The controller in that DG or energy storage is called the master controller; others are slave controller. Every slave controller will decide their operation mode based on the master controller. [4, 5]

In Figure 1.1, it shows a very simple structure of master-slave control. In this microgrid, it has central DG, DG, PV, wind turbine and load. The slave controllers use reference signal which comes from the master controller to control DG output. The master controller also controls the main DG or energy storage.

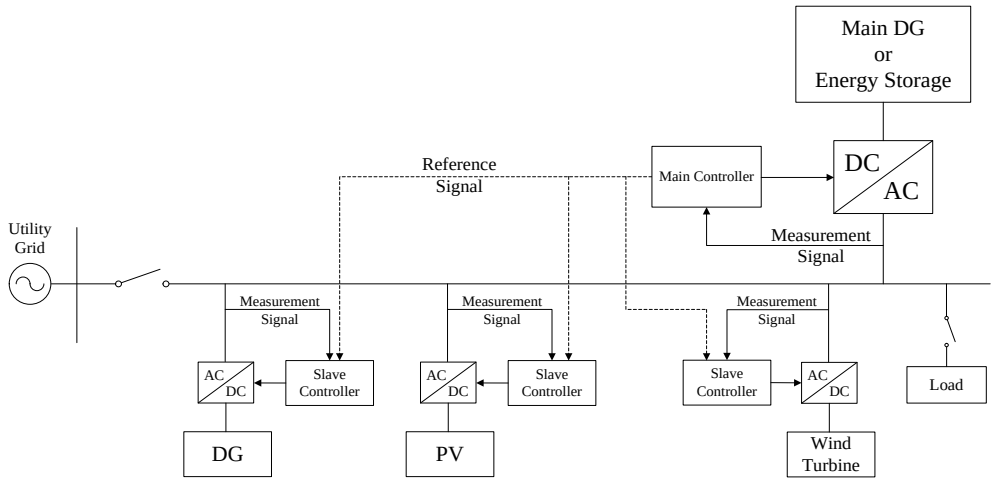

Figure 1.1 The master-slave control structure

In the peer to peer control, every controller, on equal footing, uses the measurement signal, such as voltage and frequency, at the Point of Common Coupling (PCC) to control every part of the microgrid.

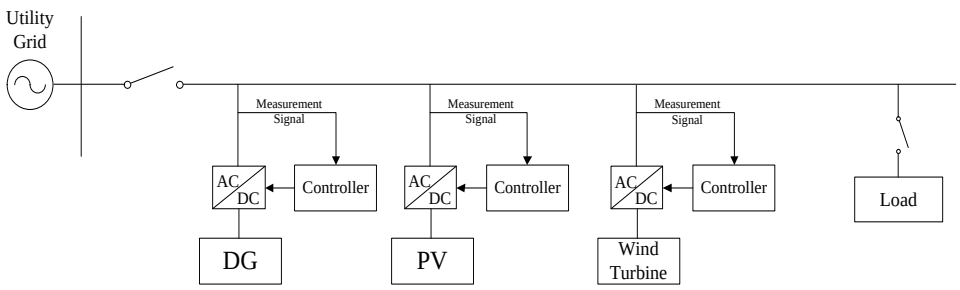

Figure 1.2 The peer to peer control structure

As shown in Figure 1.2, the controllers in the microgrid have their reference. Different controllers will not impact the reference signal in other controllers.

When the microgrid uses the hierarchic control structure, it has a central processing unit (CPU) to send the control signal to every part in microgrid [6]. By predicting the output power in every DG and load requirement, the CPU will formulate an operation plan. In the same time, it can make the real-time adjustment by collecting the voltage, current and frequency from the microgrid to make sure that the voltage and frequency are stable.

For the control objective, we have P/Q control and droop control. As we know, active and reactive power, voltage, current and frequency are critical parameters in the microgrid. We can use meters to observe those parameters to estimate whether microgrid effective performance is stable.

PV and wind turbine are used as distribution generations in the microgrid. However, they are always influenced by nature. That will cause the unstable output from

DG. Thus, people use the P/Q control in microgrid grid-connected mode to control the output power, including active and reactive power, to make sure that load can get the steady energy from DG in the microgrid.

When working in the grid-connected model, the utility grid will support the stable voltage and frequency to the microgrid. However, when operating in islanded mode, microgrid needs to support its stable voltage and frequency. Thus, the droop control is always used in the islanded model to make sure that microgrid can provide the stabilized electrical power with steady voltage and frequency for loads.

In this thesis, the droop control based on Model Predictive Control (MPC) will be used in peer to peer control structure.

1.3 Literature Review

The microgrid provides several methods for the distributed generation connecting to the utility grid. It improves the reliability of electric power supply system [7]. Meanwhile, the microgrid application can solve the power supply issue in some remote region and the loss of the transmission line can be decreased.

The control system in the microgrid is a very significant research area. In the traditional microgrid control system, the controllers based on proportional-integral-derivative (PID) are widely used. It decomposes a complex system into the single-input, single-output loop or linearizes the system around an operating

point in a slight range [8-9]. Thus, the traditional PID control strategy has limitations for the multiple-input and multiple-output (MIMO) or nonlinear control systems with constraints.

However, the model predictive control (MPC) is achieved by solving a finite horizon open-loop optimal control problem in real time. The optimization on control variables yields an optimal control variable sequence, and the first control variable in this sequence is applied to the control system [10].

The modern control concepts were started based on the Linear Quadratic Regulator (LQR) design on Kalman's work in 1960[11]. In 1978, J Richalet proposed the Model Predictive Heuristic Control (MPHC) to solve the application of the large scale industrial processes for more than a year's time [12]. Then in 1980, C.R. Cutler and B.L. Ramaker put forward the concept of Dynamic Matrix Control (DMC), a computer control algorithm, to solve the complex control problems on a digital computer which are not solvable with traditional PID control concepts [13]. Those two algorithms are the first generation of MPC, and both of them have a good effect in the control of unconstrained multivariate processing. However, the state and control constraint are not disposed of in MPHC and DMC.

After that, the second generation of MPC is proposed. In 1986, the Quadratic Dynamic Matrix Control (QDMC), to improve DMC, was present by Carlos E. Garcia

and A.M. Morshedi. In this theory, authors used a quadratic program to keep controlled variables close to their targets by computing moves on process manipulated variables when preventing violations of process constraints [14]. By using the solution of quadratic programming as the input, QDMC solves the optimal control constraint problems in open loop. However, the second generations of MPC still have some issues. They cannot solve the problem of enlarging the feasible set when the output constraints are present [15].

In the third generation, MPC can be applied in the system which has different kinds of constraints with different priority and also can solve the problem of enlarging the available set when the output constraints are present. Moreover, it can be used in various cost functions and multi−criterial optimization [15]. The Shell Multivariable Optimizing Controller (SMOC) proposed by Marquis in 1988[16] is a case of third generations. The SMOC used the state-space linear models to describe a very broad class of dynamic processes [16].

With the increasing industrial process control requirements, the traditional PID controller has been difficult to satisfy the complex industrial process. Through the research of MPC, it is widely used in the industrial community. MPC can effectively overcome the uncertainty and non-linearity of the process, and also can deal with the variables constraints in processing controlled variables and manipulated variables.

For example, in [17], the MPC is used for regulating a robust system identification. The data of temperature is collected for the control system identification. This paper shows that the MPC method is superior to current PID controllers and can be easily implemented in current digital process control computers.

However, the application of MPC in power grid is proposed in recent years. The traditional Proportion Integration Differentiation (PID) control is widely used in power system. With the increasing customer demand for electricity energy and better quality, some other control methods are starting to be used in power system.

In [18], it shows an application of hybrid MPC in DG, which are two generators; connected to the utility grid. This system combines continuous and hybrid dynamic operation mode. Depending on the power circuit structure and the fuel cell stack state, it can operate in four distinct modes. This paper successfully proposes a hybrid receding horizon finite-time optimal controller based on on-line multi-parametric programming techniques.

An auxiliary coordinated control approach focusing on transient voltage stability is proposed in [19] and [20]. By the support vector machine (SVM) using synchrophasor measurement data in the high penetration renewable power system, the voltage stability condition of the electrical system is predicted. The designed auxiliary MPC strategy will

augment the existing control variables aiming to keep transient voltage stability. The prediction results trigger the controllers.

In [21], the MPC is used to manage the energy-efficient microgrid. The issue of efficiently optimizing microgrid operations is formulated by using Mixed Integer Linear Programming (MILP) in this paper. To solve this problem, authors use the MPC method in the case study, and the simulation results present the effectiveness and feasibility of the proposed strategy.

The MPC can be used for the master generation unit to lead voltage and frequency in microgrid islanded mode. In [22], when a fault happened in the master unit, the fault tolerance is achieved by using MPC structure because of its flexibility and capability for handling constraints. The control robustness of MPC is also tested in the different operation mode of the microgrid.

1.4 Expected Contribution

In this thesis, a microgrid simulation model which uses MPC controller will be studied to complete the expected contribution as following:

(1) Realizing the MPC controller to control the active power, voltage and frequency in the microgrid simulation in MATLAB/Simulink.

(2) Comparing with the traditional PI controller and MPC controller to introduce advantages of MPC method.

(3) Using the MPC controller in some microgrid simulation cases to verify its reliability.

CHAPTER TWO: MICROGRID CONTROL STRATEGY STUDY

2.1 The Inverter of Grid-connected Microgrid Controller

The topologic structure of inverter in the three-phase grid is shown below:

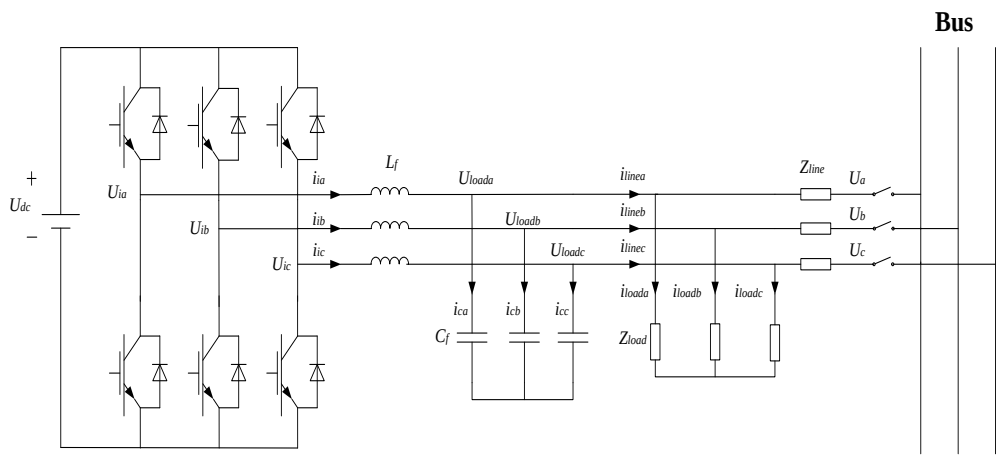

Figure 2.1 Topologic structure of inverter in three-phase grid

From the structure, we can see that the three-phase inverter is connected to the bus through filter inductance L_f, capacitance C_f and line impedance Z_{line}. The impedance of the load is Z_{load}. In this structure, the U_{ia}, U_{ib} and U_{ic} are the output three-phase voltages of the inverter. The i_{ia}, i_{ib} and i_{ic} are the output three-phase currents of the inverter, and they are also the input currents of LC filter. The i_{ca}, i_{cb} and i_{cc} are the input three-phase currents of the capacitor in LC filter. The U_{loada}, U_{loadb} and U_{loadc} are the three-phase voltages of load, and they are also the output three-phase voltages of LC

filter. The i_{linea}, i_{lineb} and i_{linec} are the three-phase currents in the transmission line. The i_{loada}, i_{loadb} and i_{loadc} are the input three-phase currents of the load. The three-phase voltages of BUS are U_a, U_b and U_c.

Thus, we can obtain voltage and current equations according to Kirchhoff's Voltage Law and Kirchhoff's Current Law:

$$\begin{cases} L_f \frac{di_{ik}}{dt} = U_{ik} - U_{loadk} \\ C_f \frac{dU_{loadk}}{dt} = i_{ik} - i_{linek} \end{cases} \tag{2.1}$$

In 2.1, the i_{ik}, i_{linek}, U_{ik} and U_{loadk} are:

$$i_k = \begin{bmatrix} i_{ia} \\ i_{ib} \\ i_{ic} \end{bmatrix},\ i_{linek} = \begin{bmatrix} i_{linea} \\ i_{lineb} \\ i_{linec} \end{bmatrix},\ U_{ik} = \begin{bmatrix} U_{ia} \\ U_{ib} \\ U_{ic} \end{bmatrix},\ U_{loadk} = \begin{bmatrix} U_{loada} \\ U_{loadb} \\ U_{loadc} \end{bmatrix}.$$

In the simulation, the functions of switches need to be defined as:

$$S_{i(i=a,b,c)} = \begin{cases} 1 \\ 0 \end{cases}$$

When $S_i = 1$, the upper bridge arms will be connected and the lower bridge arms will be opened. When $S_i = 0$, the upper bridge arms will be disconnected and, the lower bridge arms will be closed.

Thus, the output three-phase voltage of the inverter is:

$$U_{ik} = \begin{bmatrix} U_{ia} \\ U_{ib} \\ U_{ic} \end{bmatrix} = \begin{pmatrix} \frac{2}{3} & -\frac{1}{3} & -\frac{1}{3} \\ -\frac{1}{3} & \frac{2}{3} & -\frac{1}{3} \\ -\frac{1}{3} & -\frac{1}{3} & \frac{2}{3} \end{pmatrix} \begin{pmatrix} S_a \\ S_b \\ S_c \end{pmatrix} U_{dc} \tag{2.2}$$

Combining the equation 2.1 and 2.2, the mathematical model of the inverter can be described by the switch function, which is:

$$\begin{cases} L_f \frac{d}{dt}\begin{bmatrix} i_{ia} \\ i_{ib} \\ i_{ic} \end{bmatrix} = \begin{pmatrix} \frac{2}{3} & -\frac{1}{3} & -\frac{1}{3} \\ -\frac{1}{3} & \frac{2}{3} & -\frac{1}{3} \\ -\frac{1}{3} & -\frac{1}{3} & \frac{2}{3} \end{pmatrix}\begin{pmatrix} S_a \\ S_b \\ S_c \end{pmatrix} U_{dc} - \begin{bmatrix} U_{loada} \\ U_{loadb} \\ U_{loadc} \end{bmatrix} \\ C_f \frac{d}{dt}\begin{bmatrix} U_{loada} \\ U_{loadb} \\ U_{loadc} \end{bmatrix} = \begin{bmatrix} i_{ia} \\ i_{ib} \\ i_{ic} \end{bmatrix} - \begin{bmatrix} i_{linea} \\ i_{lineb} \\ i_{linec} \end{bmatrix} \end{cases} \quad 2.3$$

Hence, the mathematical model of the inverter in static three-phase coordinate, which is the *abc* reference frame system, can be obtained. However, we need to transform it to the rotary two-phase coordinate, which is the *dq* reference frame system, for designing the control system conveniently.

The transform matrix equation is:

$$\begin{bmatrix} x_d \\ x_q \end{bmatrix} = \frac{2}{3}\begin{bmatrix} \cos\omega t & \cos(\omega t - 2\pi/3) & \cos(\omega t + 2\pi/3) \\ -\sin\omega t & -\sin(\omega t - 2\pi/3) & -\sin(\omega t + 2\pi/3) \end{bmatrix}\begin{bmatrix} x_a \\ x_b \\ x_c \end{bmatrix} = T_{3s/2r} * \begin{bmatrix} x_a \\ x_b \\ x_c \end{bmatrix} \quad 2.4$$

In this equation, ω is the angular frequency in the *dq* synchronous reference frame system.

After transformation, the mathematical model of the inverter in *dq* synchronous reference frame system is shown below:

$$\begin{cases} L_f \frac{di_{id}}{dt} = U_{id} - U_{loadd} \\ L_f \frac{di_{iq}}{dt} = U_{iq} - U_{loadq} \\ C_f \frac{dU_{loadd}}{dt} = i_{id} - i_{lined} \\ C_f \frac{dU_{loadq}}{dt} = i_{iq} - i_{lineq} \end{cases} \quad 2.5$$

2.2 The LC filter

The LC filter design for the inverter which using the Sinusoidal Pulse Width Modulation (SPWM) is imperative. This modulation method will produce a lot of harmonic in the switching frequency. In the real program, people always use the LC Passive power filter to solve this problem.

The formula of LC filter design is:

$$f_c = 1/\left(2\pi\sqrt{L_f C_f}\right) \tag{2.6}$$

$$10f_n \leq f_c \leq f_s/10 \tag{2.7}$$

where f_c is the resonant frequency of LC filter, f_n is the frequency of modulating wave, and f_s is the frequency of SPWM carrier wave.

The function between filter output voltage V_{fout} and input voltage V_{fin} is:

$$G(j\omega) = \frac{V_{out}}{V_{in}} = \frac{1/j\omega C_f}{j\omega L_f + \frac{1}{j\omega C_f} + R_f} \tag{2.8}$$

Let $\omega_0 = 1/\sqrt{L_f C_f}$, $\xi = \frac{R}{2}\sqrt{\frac{C_f}{L_f}}$, we get:

$$G(j\omega) = \frac{{\omega_0}^2}{(j\omega)^2 + j\omega * 2\xi\omega_0 + {\omega_0}^2} \tag{2.9}$$

By using formula 2.7 ~ 2.9, the parameter of LC filter can be designed to make sure that the voltage drop in inductance cannot exceed the 3% value of system voltage.

2.3 Microgrid Control Strategy

The PQ controller is used in the renewable energy system, including the energy storage system, distributed generation and microgrid. When the inverter uses PQ control

strategy, the power source will output stable active and reactive power no matter what happened in voltage, frequency and load changing.

When microgrid works in the grid-connected mode, distribution generation can use PQ control; when microgrid operates in the islanded mode, the distribution generation should use the constant voltage and frequency control strategy to support the voltage and frequency for the microgrid.

2.3.1 The Active and Reactive Power Decoupling

For decoupling active power and reactive power, we use the Park Transformation; we transform the voltage from *abc* to *dq* reference frame system. Meanwhile, the voltage component at *q* axis is zero, u_q=0.

The formula of active and reactive power calculation in *dq* coordinate is shown below:

$$\begin{cases} P = u_d i_d + u_q i_q = u_d i_d \\ Q = -u_d i_q + u_q i_d = -u_d i_q \end{cases} \tag{2.10}$$

From the formula 2.10, we can easily find that the active power and reactive power can be controlled separately by adjusting i_d and i_q.

Using Kirchhoff Law and Park Transformation, we can get the relationship between voltage and current, which is:

$$\begin{cases} u_d^* = u_{loadd} + Ri_d + L\frac{di_d}{dt} - \omega L i_q \\ u_q^* = u_{loadq} + Ri_q + L\frac{di_q}{dt} + \omega L i_d \end{cases} \tag{2.11}$$

In this transformation, u_q=0, so we can get:

$$\begin{cases} u_d^* = u_{loadd} + Ri_d + L\frac{di_d}{dt} - \omega Li_q \\ u_q^* = Ri_q + L\frac{di_q}{dt} + \omega Li_d \end{cases} \quad 2.12$$

Thus, the decoupling of active power and reactive power is achieved.

2.3.2 PQ controller

Using formula 2.12, we can get the PQ controller diagram, which is shown in Figure 2.2:

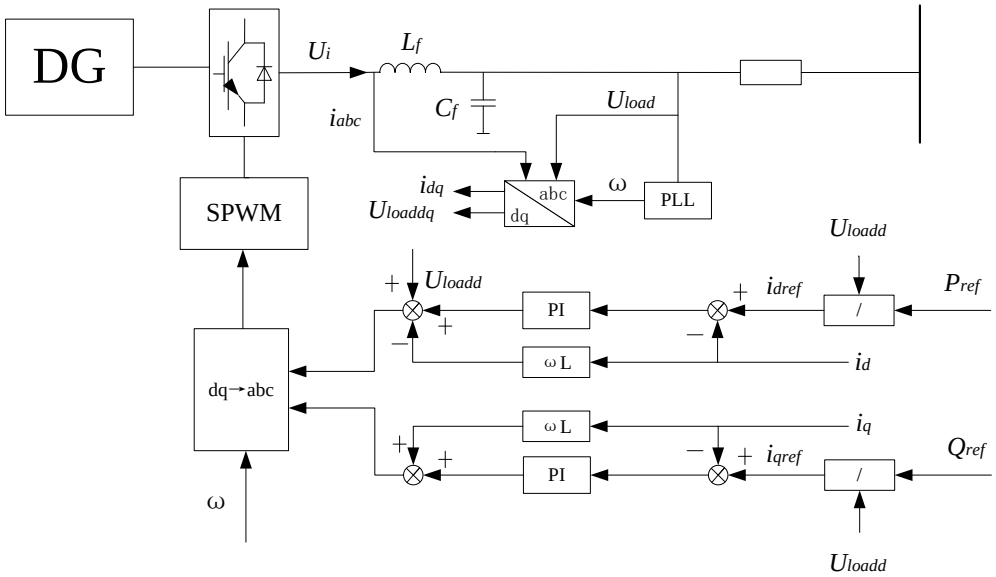

Figure 2.2 PQ controller diagram

In Figure 2.2, the reference currents in d axis and q axis are calculated from formula 2.9. The difference value between the reference current and real current will be adjusted by the PI controller and then process current feedforward compensation. Hence we get the voltage modulating signal. The signal will be modulated by the SPWM and as

a switch signal to the inverter. In this system, the system frequency can be detected by the phase-locked loop (PLL) block.

2.3.3 Droop control

In a microgrid, the current, generated by dc voltage source, will be inverted by the inverter to become three-phase current. And then pass through line impedance to the AC bus. The vector diagram of power transmission is shown in fig 2.3:

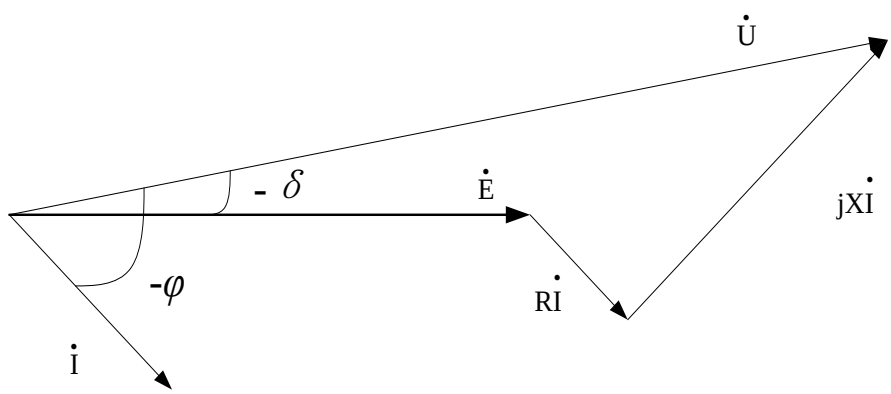

Figure 2.3 Power transmission vector diagram

In this vector diagram, U is the amplitude of output voltage from the inverter, E is the amplitude of ac bus voltage, δ is the phase angle difference between the inverter output voltage vector and ac bus voltage vector.

Then we can get the formula of inverter output:

$$S = P + jQ = \dot{E}\dot{I}$$

$$= (E\cos\delta - jE\sin\delta)\left(\frac{U - E\cos\delta + jE\sin\delta}{Z\cos\theta - jZ\sin\theta}\right)$$

$$= \frac{1}{Z}(EU\cos\delta\cos\theta - E^2\cos\theta + EU\sin\delta\sin\theta)$$

$$+j\frac{1}{Z}(EU\cos\delta\sin\theta - E^2\sin\theta + EU\sin\delta\cos\theta) \qquad 2.13$$

Thus we can get the active and reactive power of inverter output:

$$P = \left(\frac{EU}{Z}\cos\delta - \frac{E^2}{Z}\right)\cos\theta + \frac{EU}{Z}\sin\delta\sin\theta \qquad 2.14$$

$$Q = \left(\frac{EU}{Z}\cos\delta - \frac{E^2}{Z}\right)\sin\theta - \frac{EU}{Z}\sin\delta\sin\theta \qquad 2.15$$

In the low voltage system, the parameter R is much higher than X so that we can ignore the value of X. Thus $Z = R$, $\theta = 0$. Assume that the power angle δ is very small, $sin\,\delta \doteq \delta$, $cos\,\delta \doteq 1$, than we can transform 2.11 and 2.12 to:

$$P \doteq \frac{EU}{R} - \frac{E^2}{R} \qquad 2.16$$

$$Q \doteq -\frac{EU}{R}\delta \qquad 2.17$$

From formula 2.16 and 2.17, in low voltage system, the active power transmission is decided by voltage amplitude U and the reactive power transmission is decided by power angle δ.

In high voltage system, the parameter X is much greater than R so that we can ignore the value of R. Thus $Z = X$, $\theta = 90^{\circ}$. Assume that the power angle δ is very small, $sin\,\delta \doteq \delta$, $cos\,\delta \doteq 1$, than we can transform 2.11 and 2.12 to:

$$P \doteq \frac{EU}{R}\delta \qquad 2.18$$

$$Q \doteq \frac{EU}{X} - \frac{E^2}{X} \qquad 2.19$$

From formula 2.18 and 2.19, in high voltage system, the active power transmission is decided by power angle δ, and voltage amplitude U determines the reactive power transmission.

The droop characteristic curve is shown in Figure 2.4 and 2.5:

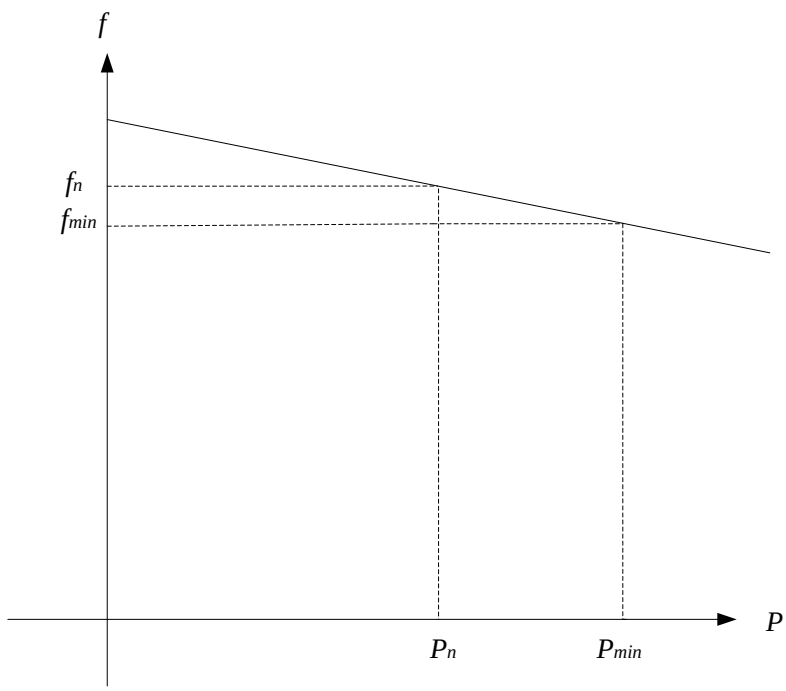

Figure 2.4 P/f droop curve

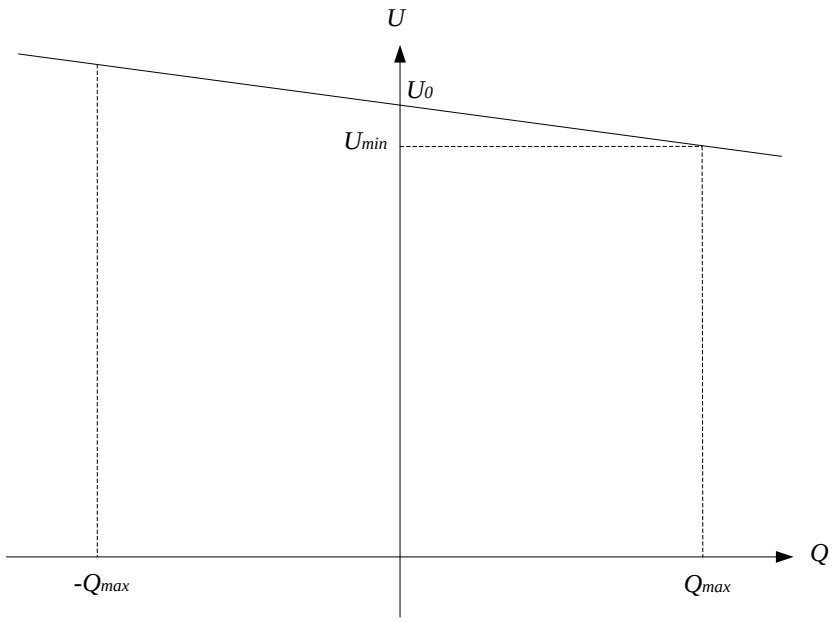

Figure 2.5 Q/U droop curve

The frequency and amplitude of inverter output voltage will be changed by their droop characteristic as follow:

$$f = f_n - m(P - P_n) \tag{2.20}$$

$$U = U_0 - nQ \tag{2.21}$$

In formula 2.20 and 2.21, $f_n$is the rated frequency. $P_n$is the output power when system working in rated frequency. $U_0$is the voltage amplitude when the reactive power from micro source is 0. *m* is the active power droop coefficient and *n* is the reactive power droop coefficient.

By using the droop controller based on P/f, Q/U droop curve, microgrid system can distribute the unbalance power to each unit dynamically to eliminate reactive current circulation.

The droop controller diagram is shown in Figure 2.6:

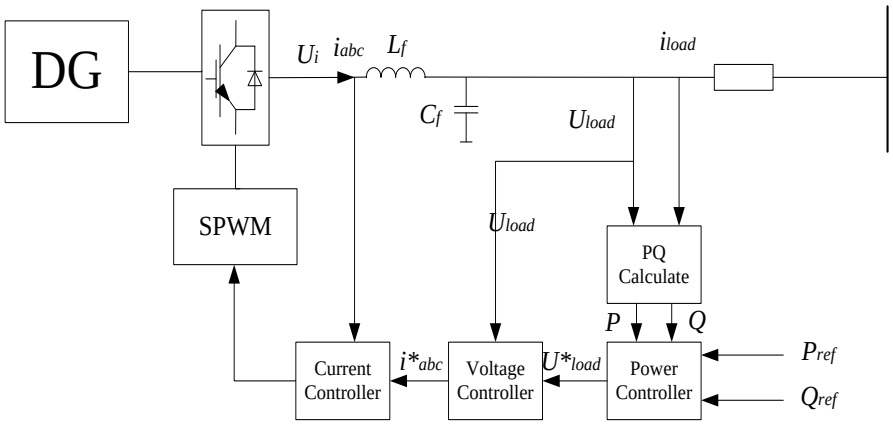

Figure 2.6 Droop controller diagram

This droop controller includes power controller and the voltage current double loop controller.

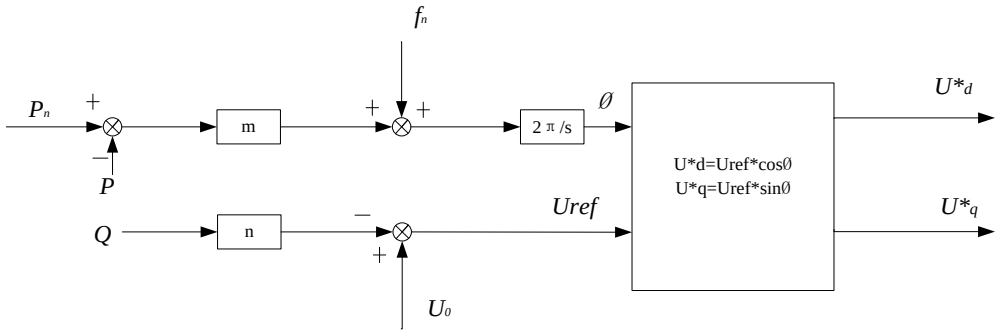

Figure 2.7 Power controller diagram

Figure 2.7 shows the power controller diagram. In this controller, f_n is the rated frequency, P_n is the active power when system frequency is f_n. U_0 is the voltage amplitude when the reactive power from micro-source is 0.

In the power controller, the frequency is used as control signal instead of phase angle. The output of power controller is the input of voltage current double loop controller. The diagram of double loop is shown in Figure 2.7.

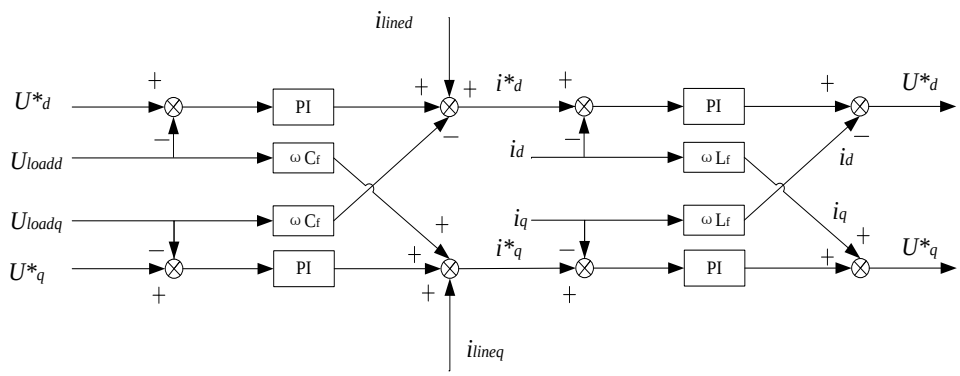

Figure 2.8 Diagram of voltage current double loop

In Figure 2.8, the outer loop is the instantaneous voltage feedback loop; the inner loop is the instantaneous current feedback loop. The difference value between the output voltage and reference voltage goes through the PI block, then as the input to the inner current loop. The current from LC filter will be compared with the reference current, then get the difference value as an error signal. The signal will go through the PI block, then as the modulation signal to SPWM. In this controller, the inner current loop can control the inductance current from the filter to improve the stability of the system.

CHAPTER THREE: MODEL PREDICTIVE CONTROL

In this chapter, an inverter control strategy is designed for the microgrid system. In every sampling period, the control variables will be evaluated by the established prediction model, and the minimal value of control variable in the function will be chosen for the next sampling period.

This control strategy ellipsis the current linear controller and PWM. Thus, it can be quickly realized by the digital signal processor.

3.1 Principle of Model Predictive Control (MPC)

The principle of model predictive is shown in Figure 3.1. $S(t)$ is the gating signal to control power electronic inverter. T_s is the defined sampling period.

In this principle diagram, $x(t)$ is the system state variables. At time t_k, the system state is $x(t_k)$. It is assumed that there are n kinds of control variables that can control the system, and n are finite. S_i (i=1, . . , n) is defined as the system control variable. According to the state variable $x(t)$ and predictive function f, all of the state variables, $x_i(t_{k+1}) = f\{x(t_k), S_i\}, i = 1, \dots, n$, can be predicted at time t_k. The predictive function can be of any form as long as the predictive function can be applied to model predictive control strategies. The function f can be deduced by the system discretization

model and its parameters.

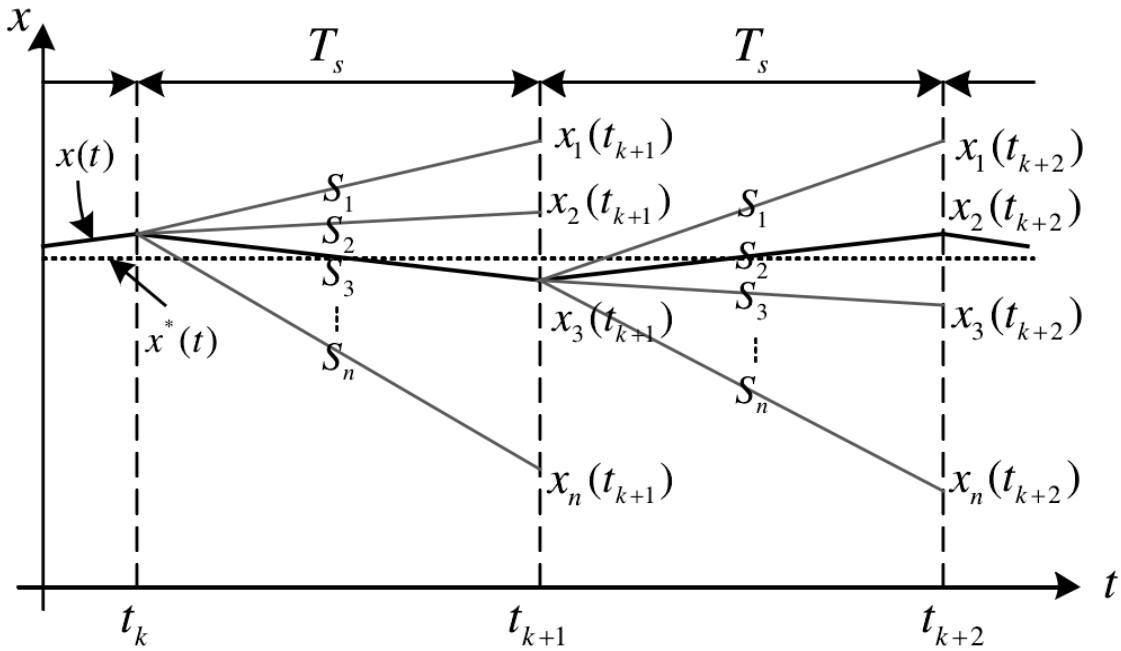

Figure 3.1 Principle of model predictive control

A function f_g is defined to determine the optimal control behavior at a certain time. f_g is consisted by reference variable, $x^*(t)$,and predictive state variable, $x_i(t_{k+1})$, which is: $g_i = f_g\{x^*(t), x_i(t_{k+1})\}, i = 1, \dots, n$.The common function is square of the difference between the reference variable and predictive state variable, which is $g_i = x^*(t) - x_i(t_{k+1})^2$. At a certain time, n values of the control variable in the system will lead the function to get n different value, g_i.

The Figure 3.1 shows that at time $t = t_k$, the control variable S_3 make the value function g_i to minimum. Hence S_3 is chosen at time $t = t_k$; at time $t = t_{k+1}$, the control variable S_2 make the value function g_i to minimum. Hence S_2 is chosen at

time $t = t_{k+1}$. The system will use this method to select the control variable in the future control period.

3.2 MPC Controller

3.2.1 PQ controller with MPC

According to the Kirchhoff's Law, the formula of three-phase voltage and current from inverter can be confirmed:

$$L_f \frac{d}{dt}\begin{bmatrix} i_a \\ i_b \\ i_c \end{bmatrix} = \begin{bmatrix} U_{ia} \\ U_{ib} \\ U_{ic} \end{bmatrix} - \begin{bmatrix} U_{loada} \\ U_{loadb} \\ U_{loadc} \end{bmatrix} \tag{3.1}$$

Then transform this formula to the *α*-*β* reference frame system, we get:

$$L_f \frac{d}{dt}\begin{bmatrix} i_\alpha \\ i_\beta \end{bmatrix} = \begin{bmatrix} U_{i\alpha} \\ U_{i\beta} \end{bmatrix} - \begin{bmatrix} U_{load\alpha} \\ U_{load\beta} \end{bmatrix} \tag{3.2}$$

After discretizing, we get:

$$\frac{L_f}{T_s}\begin{bmatrix} i_\alpha(k+1) - i_\alpha(k) \\ i_\beta(k+1) - i_\beta(k) \end{bmatrix} = \begin{bmatrix} U_{i\alpha}(k) \\ U_{i\beta}(k) \end{bmatrix} - \begin{bmatrix} U_{load\alpha}(k) \\ U_{load\beta}(k) \end{bmatrix} \tag{3.3}$$

where T_s is the sampling period. Then we get:

$$\begin{bmatrix} i_\alpha(k+1) \\ i_\beta(k+1) \end{bmatrix} = \begin{bmatrix} i_\alpha(k) \\ i_\beta(k) \end{bmatrix} + \frac{T_s}{L_f}\begin{bmatrix} U_{i\alpha}(k) - U_{load\alpha}(k) \\ U_{i\beta}(k) - U_{load\beta}(k) \end{bmatrix} \tag{3.4}$$

Using the switch function, we obtain the formula of the inverter voltage in *α*-*β* reference frame system:

$$\begin{cases} U_{i\alpha} = \sqrt{\frac{2}{3}} U_{dc}\left[S_a - \frac{1}{2}(S_b + S_c)\right] \\ U_{i\beta} = \frac{\sqrt{2}}{2} U_{dc}(S_b - S_c) \end{cases} \tag{3.5}$$

After transforming the predictive current and voltage to dq reference frame system, we get:

$$\begin{bmatrix} i_d(k+1) \\ i_q(k+1) \end{bmatrix} = \begin{bmatrix} \cos\omega t & \sin\omega t \\ -\sin\omega t & \cos\omega t \end{bmatrix} \begin{bmatrix} i_\alpha(k+1) \\ i_\beta(k+1) \end{bmatrix} \quad 3.6$$

$$\begin{bmatrix} U_{loadd}(k+1) \\ U_{loadq}(k+1) \end{bmatrix} = \begin{bmatrix} \cos\omega t & \sin\omega t \\ -\sin\omega t & \cos\omega t \end{bmatrix} \begin{bmatrix} U_{load\alpha}(k+1) \\ U_{load\beta}(k+1) \end{bmatrix} \quad 3.7$$

And the ω is the angular frequency of grid.

The active and reactive power of inverter in dq reference frame system is:

$$\begin{cases} P = U_{loadd} i_d + U_{loadq} i_q = U_{loadd} i_d \\ Q = U_{loadq} i_d - U_{loadd} i_q = -U_{loadd} i_q \end{cases} \quad 3.8$$

By using the Lagrange extrapolation, the predictive formula will be:

$$U_{loadd}(k+1) = 3U_{loadd}(k) - 3U_{loadd}(k-1) + 2U_{loadd}(k-2) + U_{ref} \quad 3.9$$

Using formula 3.9, we can get the predictive value of active and reactive power, which is:

$$\begin{cases} P(k+1) = U_{loadd}(k+1) i_d(k+1) \\ Q(k+1) = -U_{loadd}(k+1) i_q(k+1) \end{cases} \quad 3.10$$

Thus, the value function is:

$$g = [P^*(k+1) - P(k+1)]^2 + [Q^*(k+1) - Q(k+1)]^2 \quad 3.11$$

In the formula 3.11, $P^*(k+1)$ and $Q^*(k+1)$ are the reference value of active power and reactive power at time $t = k+1$.

The diagram of this MPC controller is shown in Figure 3.2.

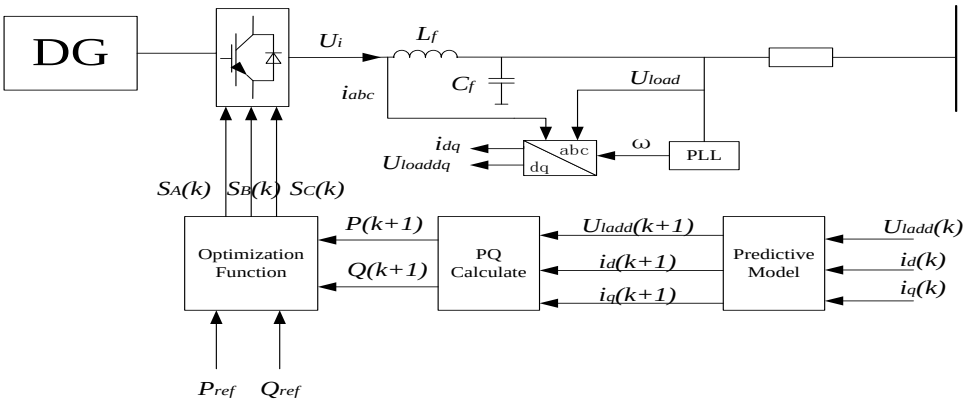

Figure 3.2 PQ controller based on MPC

Figure 3.3 is the flow chart of this MPC control.

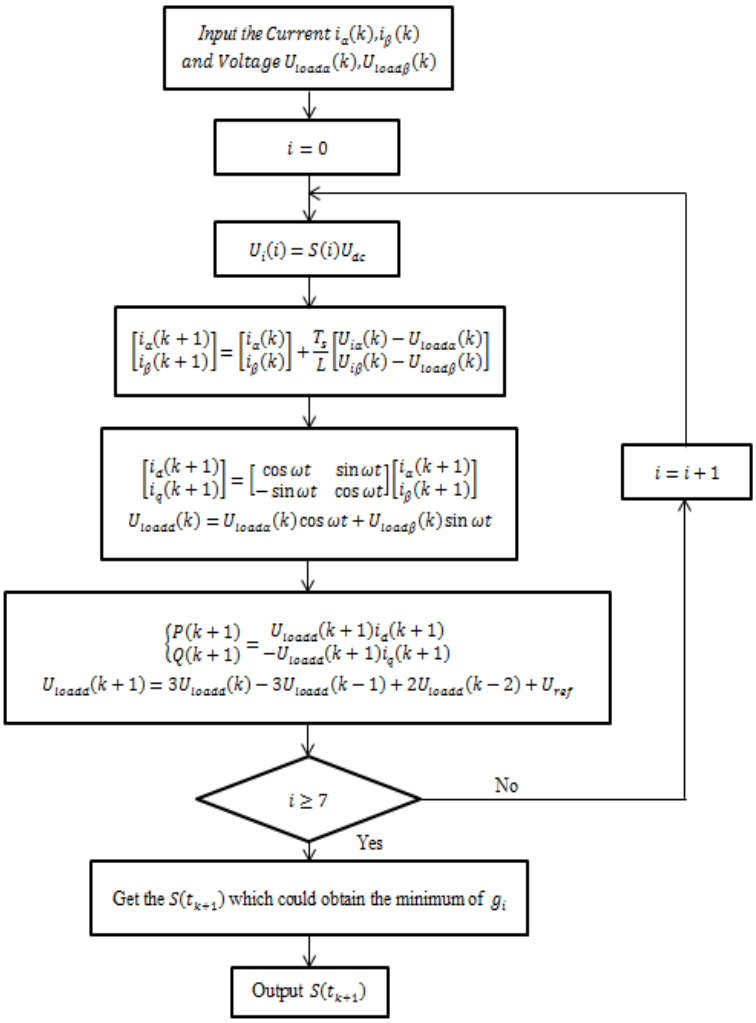

Figure 3.3 MPC controller flow chart

3.2.2 Droop controller with MPC

In MPC controller based on droop control, the current and voltage predictive model is the same as PQ controller with MPC. The voltage controller and power controller is the same as droop controller based on PI control.

The diagram of this controller is shown in Figure 3.4.

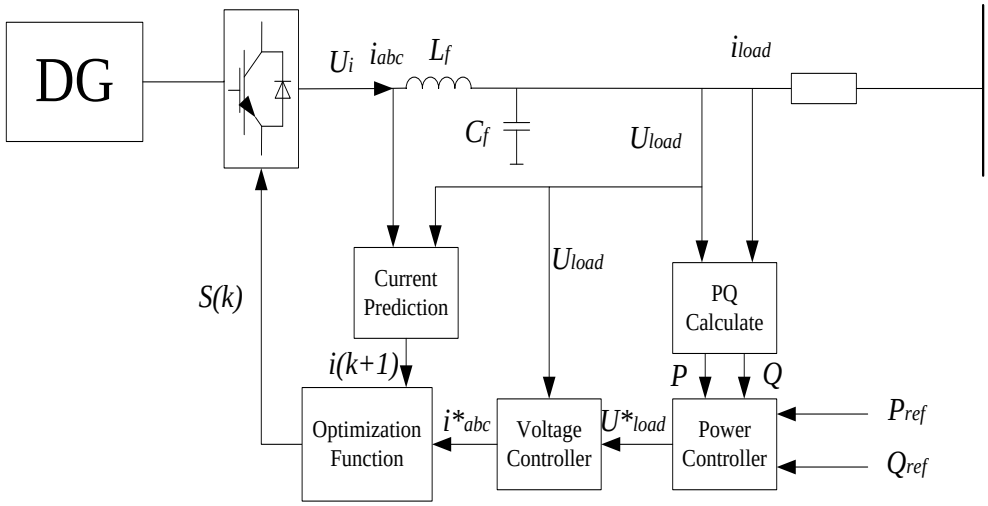

Figure 3.4 Droop controller based on MPC

3.3 The MPC Controller Model Simulation

3.3.1 PQ MPC controller simulation

The simulation diagram of one source with PQ MPC controller is shown in Figure 3.5.

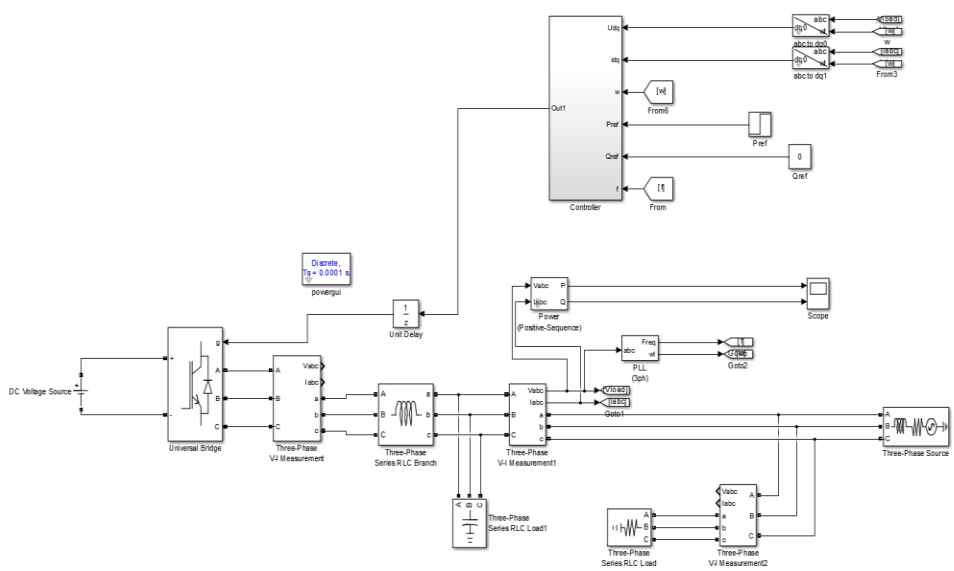

Figure 3.5 Diagram of one source with MPC controller in grid-connected mode

This diagram includes PQ controller based on MPC, *abc* to *dq* reference frame system transformation, phase locked loop (PLL) block, active and reactive power detection block. The voltage and current from micro source will be inverted and then goes into the load and utility grid.

3.3.2 Droop MPC controller simulation

The simulation diagram of one source with droop MPC controller is shown in Figure 3.6.

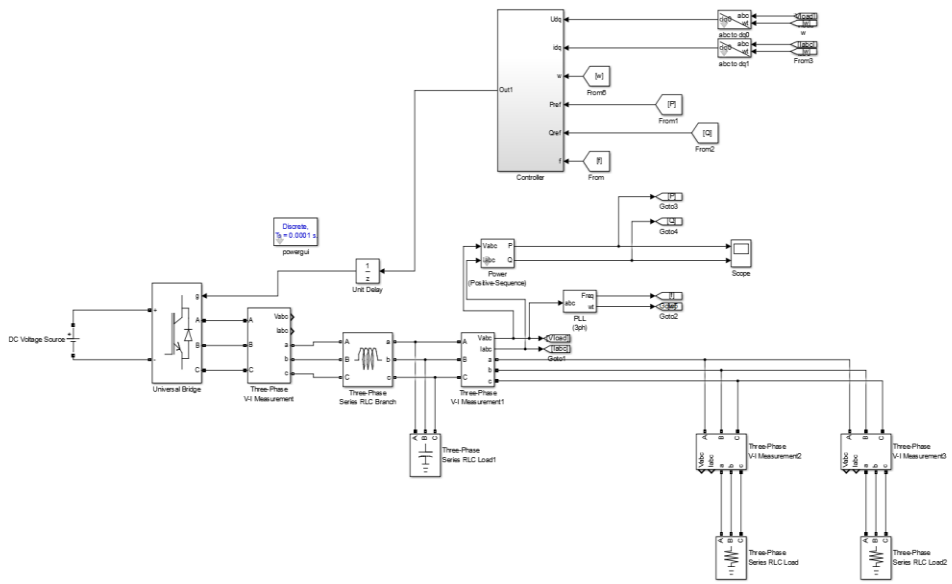

Figure 3.6 Diagram of one source with MPC controller in islanded mode

This diagram includes droop controller based on MPC, *abc* to *dq* reference frame system transformation, phase locked loop (PLL) block, active and reactive power

detection block. The voltage and current from micro source will be inverted and then goes into the load and utility grid.

3.3.3 Simulation result

3.3.3.1 PQ controller

For verifying this control strategy, the simulation model is built in the MATLAB/ Simulink. The PI control and MPC control are compared in this example. The parameters in this model are shown in Table 3.1.

Table 3.1The parameters in PQ controller

Parameter	Value
Rated Power of Source	10kW
Rated DC Voltage of Source	1000V
Microgrid Voltage	380V
Frequency	60Hz
Inductance of LC filter	0.6mH
Capacitance of LC filter	1500μF
K_p	0.5
K_i	20
Sampling Period	100μs

Two simulation cases are used to verify the decoupling of those two controllers.

In case 1, the reference value active power of distributed generator is changed from 8kW to 10kW at time t=4s and back to the 8kW at time t=6s. During this time, the reference reactive power is keeping at Q_{ref}=0. The results are shown in Figure 3.7 and 3.8. The blue line is the MPC output, and orange line is the PI output.

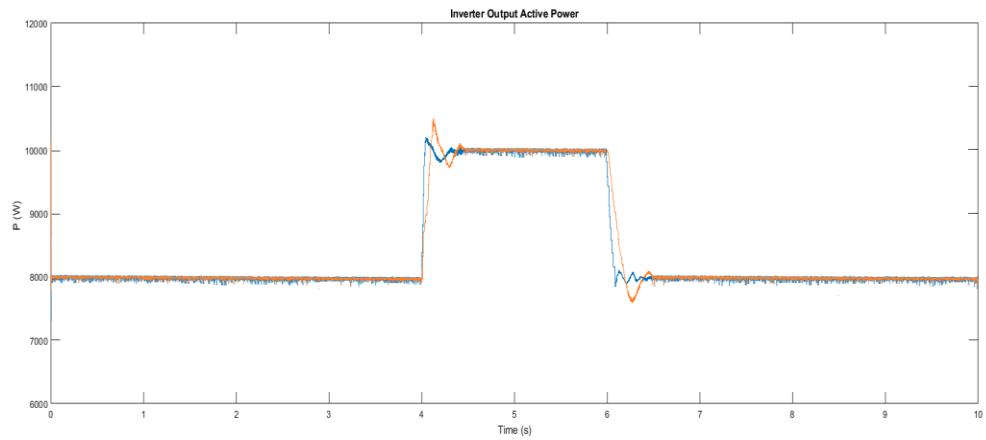

Figure 3.7 the active power of inverter output with two controllers in case 1

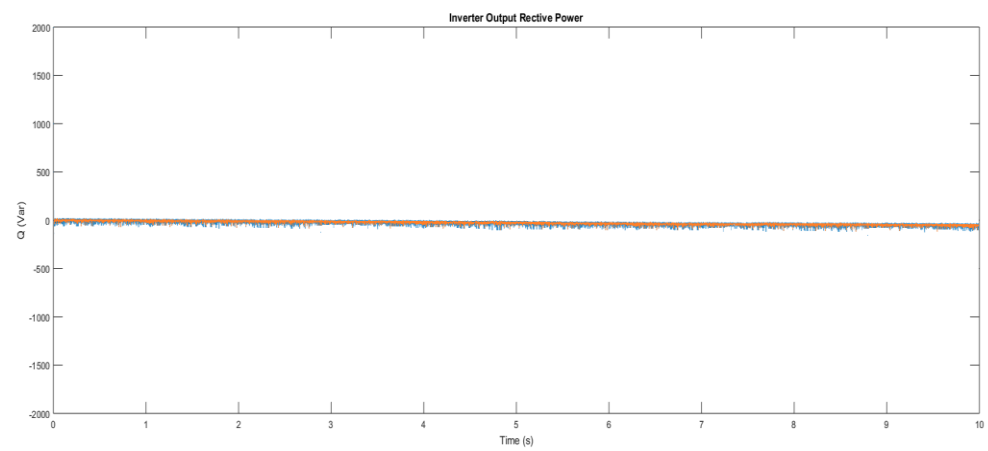

Figure 3.8 the reactive power of inverter output with two controllers in case 1

In case2, the reference reactive power of distributed generator is changed from 0kVar to 1.5kVar at time t=4s and back to the 0kVar at time t=6s. During this time, the

reference value of active power is keeping at P_{ref}=8 kW. The results are shown in Figure 3.9 and 3.10. The blue line is the MPC output, and orange line is the PI output.

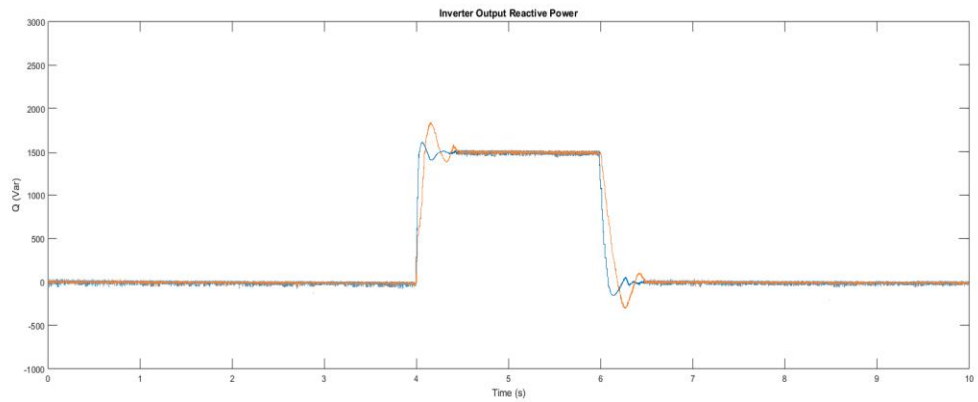

Figure 3.9 the reactive power of inverter output with two controllers in case 2

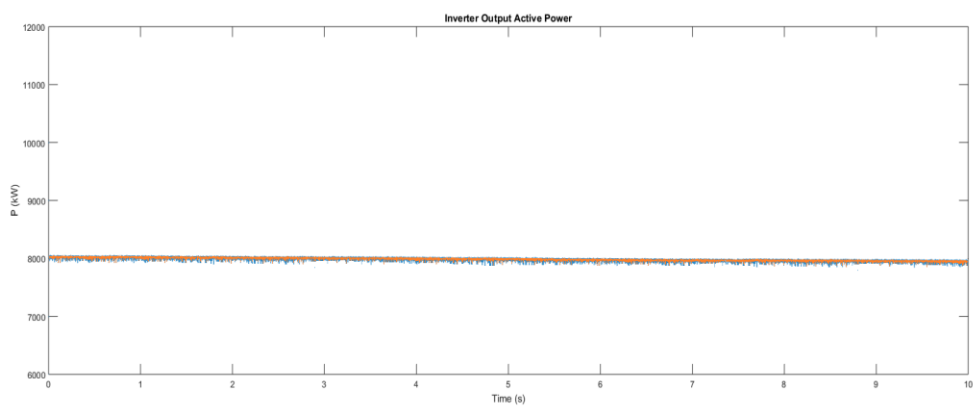

Figure 3.10 the active power of inverter output with two controllers in case 2

From Figure 3.7 and 3.9, we can find that when microgrid using the MPC controller, the overshoot is less than using a PI controller, and it has a fast response speed. It is very useful to restrain the imbalance wave in short time.

Compare with Figure 3.7 and 3.8, Figure 3.9 and 3.10, we can find that when the reference active (reactive) power changes, the reactive (active) power has no obviously wave. This case illustrates the result of decoupling in both two controllers.

The case 1 and case 2 both show that MPC control strategy has its advantage in the microgrid.

3.3.3.2 Droop controller

Two distributed generators with two controllers are built in the MATLAB/ Simulink. The parameters in this model are shown in Table 3.2.

Table 3.2The parameters in droop controller

Parameter	Value
Rated DC Voltage of Source	1000V
Rated Active Power of Source	30kW
Rated Reactive Power of Source	80kVar
Microgrid Voltage	380V
Frequency	60Hz
Inductance of LC filter	0.6mH
Capacitance of LC filter	1500μF
K_p	12
K_i	100

Load 1 Active Power	29kW
Load 1 Reactive Power	4kVar
Load 2 Active Power	10kW
Load 2 Reactive Power	4kVar
Sampling Period	100μs

In this case, case 3, the inverter controller uses droop control method. At time t=4s, load 2 is disconnected to the microgrid, and it is connected at time t=6s. The result is shown in Figure 3.11. The blue line is the MPC output, and the orange line is the PI output.

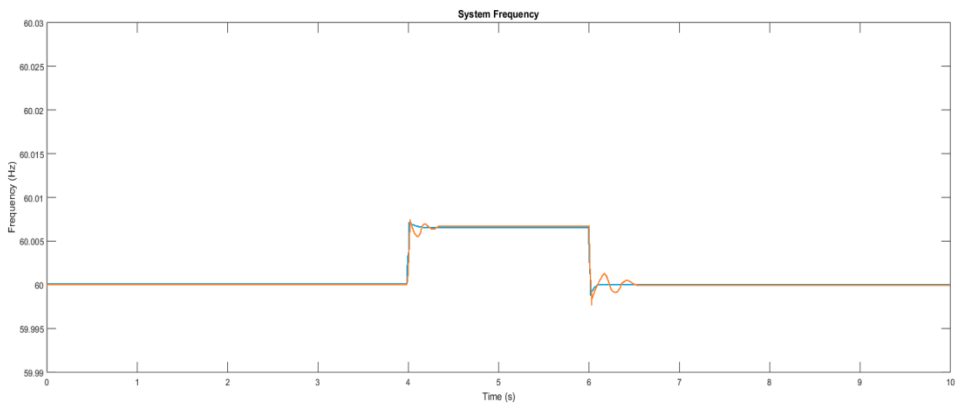

Figure 3.11The frequency response in case 3

From Figure 3.11, we can find that the MPC controller has less overshoot and fast response speed. It shows the advantage of current control by MPC controller and confirms the effect of MPC controller.

CHAPTER FOUR: CASE STUDY

For verifying the effectiveness of MPC control strategy, microgrid should work in a different mode. In this chapter, the microgrid working mode includes:

1. Microgrid model switches between grid-connected and islanded mode;

2. Increase and decrease load in islanded mode;

3. Disconnect one PV system at a certain time in islanded mode.

By simulating those three cases, the MPC controller will be verified in MATLAB/Simulink.

4.1 The Microgrid Model and Parameters

The diagram of microgrid model in MATLAB/Simulink is shown in Figure 4.1.

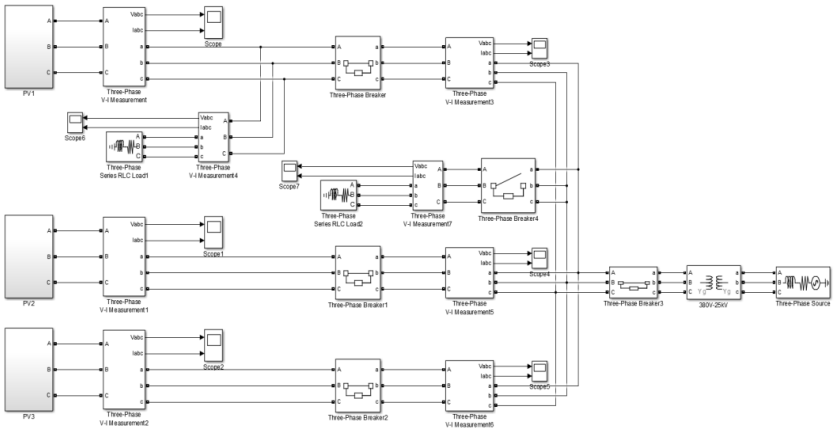

Figure 4.1 Microgrid Diagram

Figure 4.1 Microgrid DiagramIt consists of three PV models and two load blocks. The three-phase source is used to model the utility grid. When working in grid-connected mode, three PV generators are using the PQ control strategy based on MPC to make sure that the output active and reactive powers are stable. When working in islanded mode, the PV1 will use the droop control strategy based on MPC to stabilize the voltage on the bus. Both PV2 and PV3 are still using the PQ control strategy based on MPC to output constant power. The parameters of this model are shown in Table 4.1, Table 4.2 and Table 4.3.

Table 4.1 PV source parameters.

Source	Active Power (kW)	Reactive Power (kVar)
PV1	12	0
PV2	4	0
PV3	4	0

Table 4.2 Microgrid parameters

Load	Active Power (kW)	Reactive Power (kVar)
Load1	15	1
Load2	6	1

Table 4.3 Load parameters

Parameter	Value
Rated DC Voltage of Source	800V
Bus Voltage	380V
Frequency	60Hz
Inductance of LC filter	0.6mH
Capacitance of LC filter	1500μF
Lind Resistance	0.642 Ω /m
Line Inductance	0.083F/m
Droop Coefficient *a*	10^-5
Droop Coefficient *b*	3*10^-4
Sampling Period	100μs

4.2 Microgrid Model Simulation

4.2.1 Working model switches between grid-connected and islanded mode

In the simulation, the system works in grid-connected mode from the initial state to time *t=4s*; the system operates in islanded mode from *t=4*s to *t=6*s; then the system works in grid-connected mode from *t=6s* to *t=10s*.

Figure 4.2.1.1 shows active power from three PV blocks; Figure 4.2.1.2 shows reactive power from three PV blocks; Figure 4.2.1.3 shows the voltage on the bus; Figure 4.2.1.4 shows system frequency. The red line is the PV1 output, the blue line is the PV2 output, and the orange line is the PV3 output.

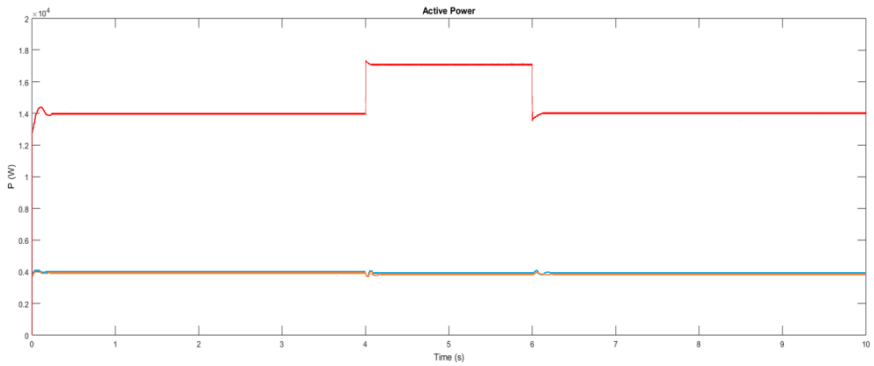

Figure 4.2.1.1 Active power of three PV

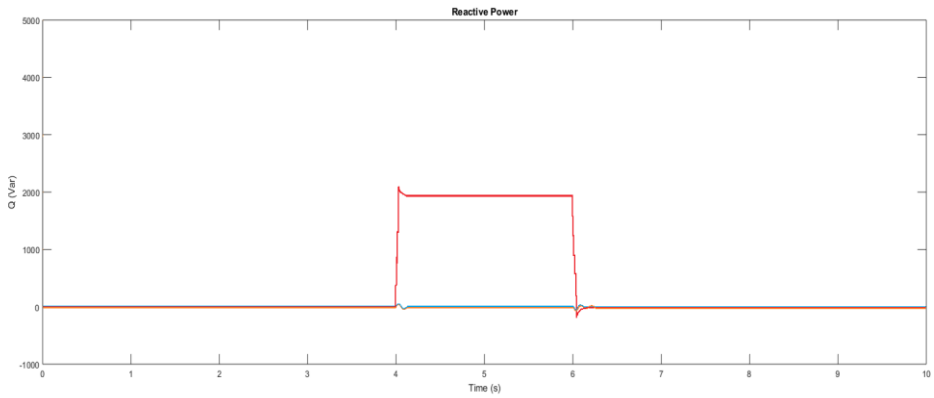

Figure 4.2.1.2 Reactive power of three PV

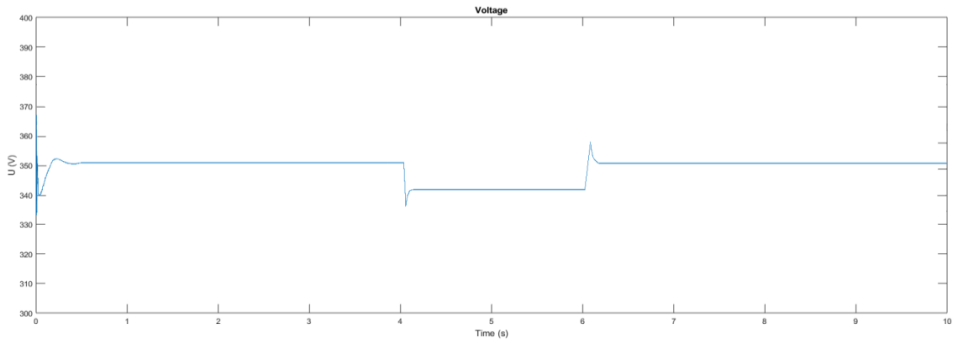

Figure 4.2.1.3 Bus voltage

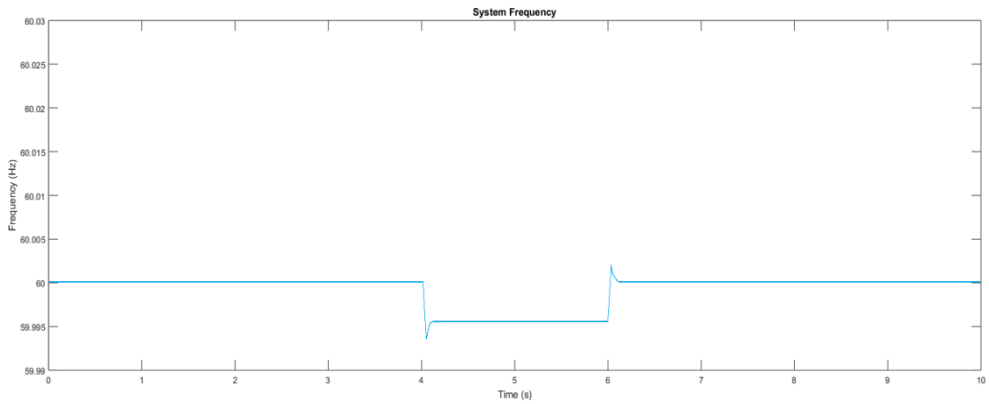

Figure 4.2.1.4 System frequency

From Figure 4.2.1.1 and 4.2.1.2, we can see that when microgrid works in grid-connected mode, the active and reactive powers from three PV generations are constant. It shows that the PQ control strategy based on MPC can achieve the expected behavior. From time t=4s to t=6s, microgrid works in islanded mode, and PV1 use the droop control strategy based on MPC. We can see that the active power and reactive power from PV1 are increased. It shows that the droop MPC controller can control the PV source, based on droop coefficient and capacity, to share power which comes from

utility grid to microgrid. In Figure 4.2.1.3 and 4.2.1.4, the bus voltage and frequency decrease when microgrid works in islanded mode and return to the standard value after microgrid connects to the utility grid. It satisfies the droop control theory. In this simulation, the bus voltage and frequency variations are in allowed range.

4.2.2 Increase and decrease load in islanded mode

In the simulation, the system works in islanded mode from the initial state to time *t=4s*; disconnect Load 2 from *t=4*s to *t=6*s; connect Load 2 from *t=6s* to *t=10s*.

Figure 4.2.2.1 shows active power from three PV blocks; Figure 4.2.2.2 shows reactive power from three PV blocks; Figure 4.2.2.3 shows the voltage on the bus; Figure 4.2.2.4 shows system frequency. The red line is the PV1 output, the blue line is the PV2 output, and the orange line is the PV3 output.

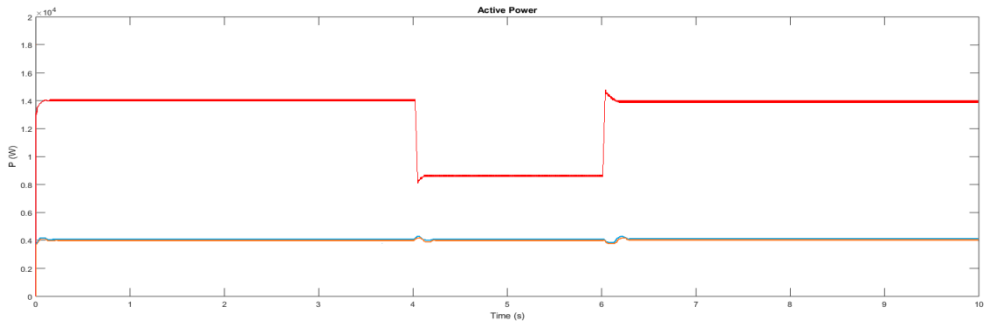

Figure 4.2.2.1 Active power of three PV

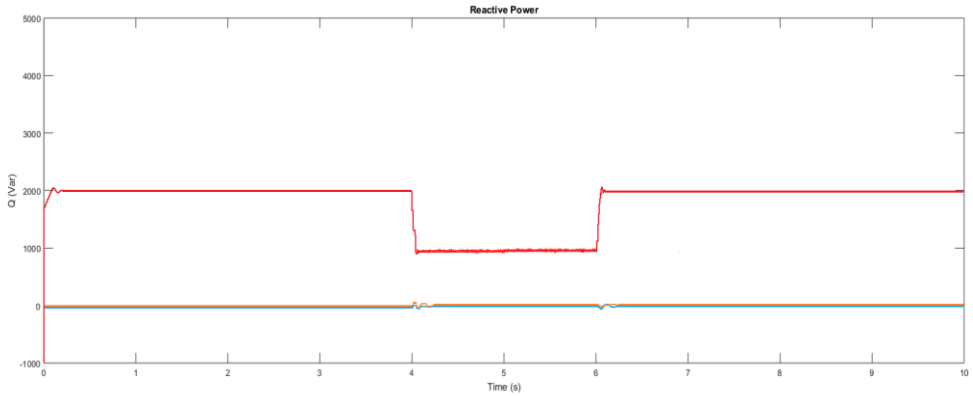

Figure 4.2.2.2 Reactive power of three PV

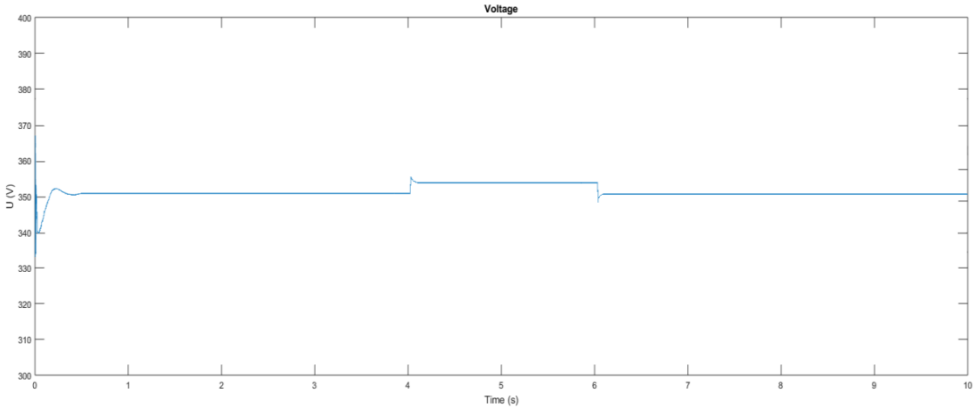

Figure 4.2.2.3 Bus voltage

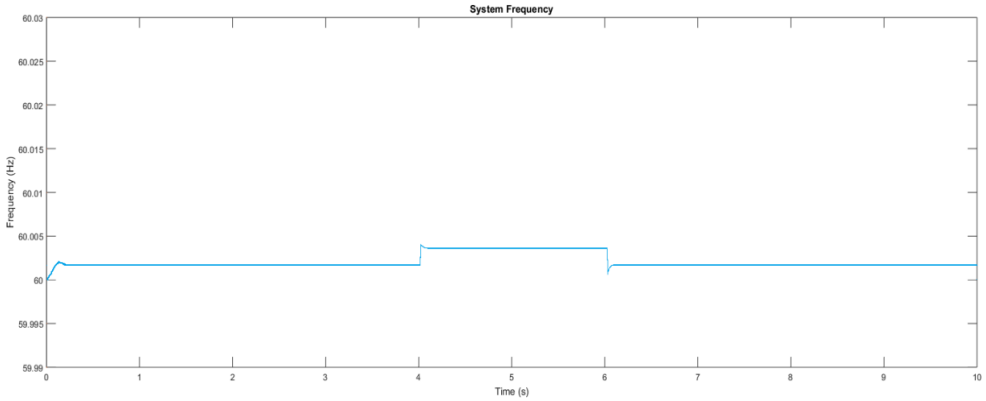

Figure 4.2.2.4 System frequency

From Figure 4.2.2.1 and 4.2.2.2, we can see that when Load2 is disconnected, the output value of active power and reactive power from PV1 are decreased. At time t=6s, the Load2 is connected to the microgrid, and then PV1 increases its output active and reactive power. It shows that when microgrid using droop MPC controller, the system will adjust the PV source output power based on its droop coefficient to achieve system balance when the load is changed. From Figure 4.2.2.3 and 4.2.2.4, the bus voltage changes following PV1 output reactive power; the frequency changes with PV1 output active power. Those phenomena show that in this control strategy, the frequency is adjusted by the active power based on P-f droop characteristic and voltage is modified by the reactive power based on Q-V droop characteristic. In this simulation case, the bus voltage and frequency variations are in allowed range.

4.2.3 Disconnect one PV system at a certain time in islanded model.

In this simulation, the system works in islanded mode from the initial state to time *t=4s*; disconnect PV2 from *t=4*s to *t=10*s.

Figure 4.2.3.1 shows active power from three PV blocks; Figure 4.2.3.2 shows the voltage on the bus; Figure 4.2.3.3 shows system frequency.

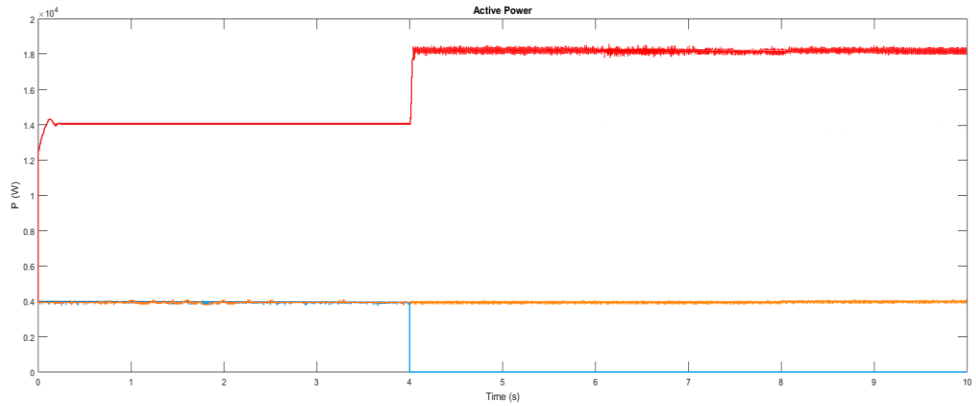

Figure 4.2.3.1 Active power of three PV

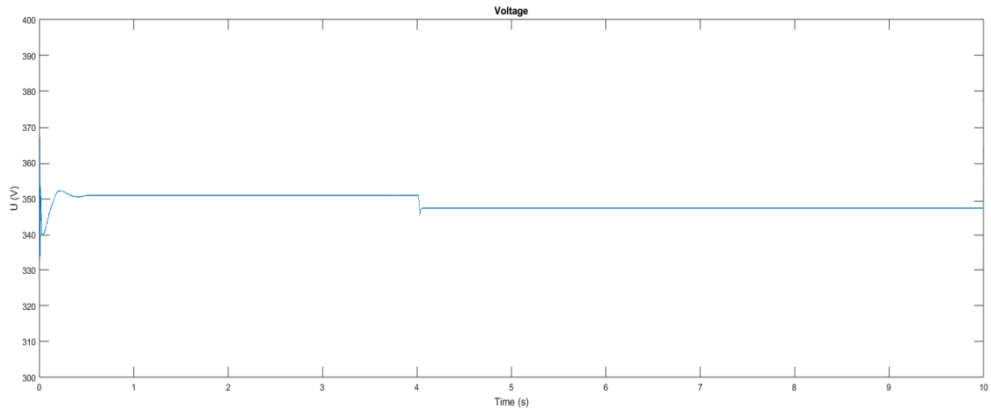

Figure 4.2.3.2 Bus voltage

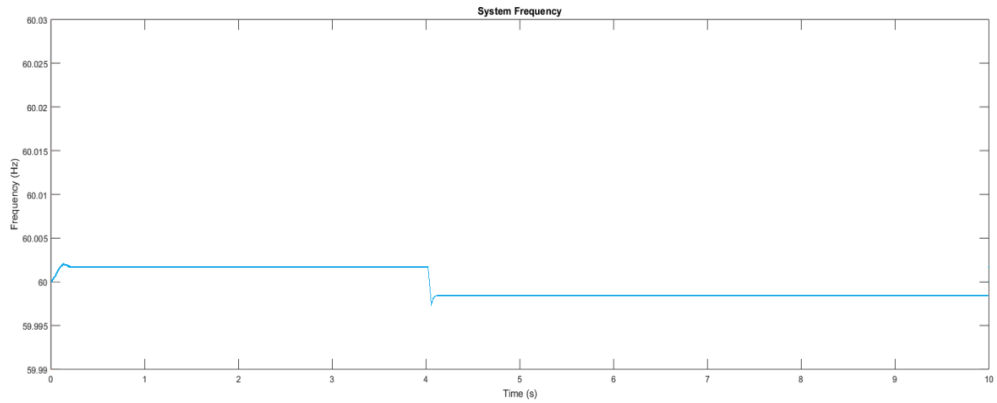

Figure 4.2.3.3 System frequency

In Figure 4.2.3.1, when PV2 is disconnected to the microgrid, PV1 can adjust its output power proportionately by itself based on the droop coefficient to achieve the system power balance. Figure 4.2.3.1 and 4.2.3.3 show that the microgrid system can supply the voltage and frequency to the whole system when some sources are disconnected.

4.3 Discussion

By analyzing the results of the three case studies, the following conclusions can be obtained:

(1) By using the droop characteristic Droop controller based on MPC, the PV1 can adjust the output power efficiently when microgrid work in the mode switching, load changing and PV source are changing in islanded mode.

(2) This control strategy can supply the voltage and frequency to microgrid system and let the voltage and frequency variations are in the allowed range.

(3) By using PQ controller based on MPC, the PV2 and PV3 can keep their output power stable and adjust the output efficiency by the control command.

CHAPTER FIVE: CONCLUSION AND FUTURE WORK

5.1 Conclusion

In this thesis, the microgrid coordination control strategy is studied by analysis the current microgrid situation and different control strategies. By using theoretical analysis and model simulation, the control strategy which proposed in this thesis is confirmed. The main component and conclusion are as follows:

(1) Design the PQ controller and droop controller, which are both based on PI control. Design the LC filter for the inverter output.

(2) MPC method is used to avoid the disadvantage of PI controller, then the PQ and Droop controller are designed based on MPC method to control the inverter output in micro-source.

(3) Building simulation models in MATLAB/Simulink to compare the PI and MPC method. The MPC controller has verified that it has better control results.

(4) A microgrid model which has three PV blocks is built in MATLAB/Simulink. Three cases are simulated in this model: 1) Working model switches between grid-connected and islanded mode; 2) Increase and decrease load in islanded mode; 3) Disconnect one PV system at a certain time in islanded mode.

(5) Through the simulation analysis, the MPC controller in microgrid system can achieve the excepted object: control the output power from inverter; share the load power. Also, voltage and frequency are controlled in the allowed band. The effectiveness of MPC control strategy is confirmed.

1.1. Future Work

This thesis conducts a validation process for microgrid control from theory to simulation. However, there still has come limitations and need to do future research.

(1) In this thesis, the simulation model only has PV micro-source. However, in the real microgrid system, some other micro-sources are widely used, such as wind turbine. Meanwhile, the battery storage system is utilized in the real microgrid system. For my future work, those two blocks will be built in my simulation model.

(2) The MPC controller which is proposed in this thesis is designed for the limit step system. For the more precise model, the control strategy needs to be studied.

REFERENCES

[1] Lasseter R, Akhil A, Marnay C, et al. The CERTS microgrid concept[J]. White paper for Transmission Reliability Program, Office of Power Technologies, US Department of Energy, 2002, 2(3): 30.

[2] Lasseter R H, Piagi P. Control and design of microgrid components[J]. PSERC Publication 06, 2006, 3.

[3] Chengshan Wang. Analysis and Simulation Theory of Microgrids. 2013.

[4] Wang Y, Lu Z, Min Y, et al. Small signal analysis of microgrid with multiple micro sources based on reduced order model in islanded operation[C]//2011 IEEE Power and Energy Society General Meeting. IEEE, 2011: 1-9.

[5] Miao Z, Domijan A, Fan L. Investigation of microgrids with both inverter interfaced and direct AC-connected distributed energy resources[J]. IEEE Transactions on Power Delivery, 2011, 26(3): 1634-1642.

[6] Funabashi T, Fujita G, Koyanagi K, et al. Field tests of a microgrid control system[C]//Proceedings of the 41st International Universities Power Engineering

[7] Conference. IEEE, 2006, 1: 232-236.[7]Lasseter R H, Eto J H, Schenkman B, and et al. CERTS microgrid laboratory test bed [J]. IEEE Transaction on Power Delivery, 2011, 26(1):325-332.

[8] Ang K H, Chong G, Li Y. PID control system analysis, design, and technology[J]. IEEE transactions on control systems technology, 2005, 13(4): 559-576.

[9] Karl J Å, Hägglund T. PID controllers: theory, design and tuning[J]. 1995.

[10] Qin S J, Badgwell T A. A survey of industrial model predictive control technology[J]. Control engineering practice, 2003, 11(7): 733-764.

[11] Nunes G C. Design and analysis of multivariable predictive control applied to an oil-water-gas separator: A polynomial approach[D]. University of Florida, 2001.

[12] Richalet J, Rault A, Testud J L, et al. Model predictive heuristic control: Applications to industrial processes[J]. Automatica, 1978, 14(5): 413-428.

[13] Cutler C R, Ramaker B L. Dynamic matrix control?? A computer control algorithm[C]//joint automatic control conference. 1980 (17): 72.

[14] Garcia C E, Morshedi A M. Quadratic programming solution of dynamic matrix control (QDMC)[J]. Chemical Engineering Communications, 1986, 46(1-3): 73-87.

[15] Ławryńczuk M. Computationally efficient model predictive control algorithms[J]. A Neural Network Approach, Studies in Systems, Decision and Control, 2014, 3.

[16] Marquis P, Broustail J P. SMOC, a bridge between state space and model predictive controllers: application to the automation of a hydrotreating unit[C]//Proceedings of the IFAC workshop on model based process control. 1988, 82: 37-43.

[17] Gustafson D E, Lebow W M. Model predictive control (MPC) of injection molding machines[C]//Decision and Control, 1987. 26th IEEE Conference on. IEEE, 1987, 26: 2017-2026.

[18] Jiang H, Zhang J J, Gao D W. Fault localization in smart grid using wavelet analysis and unsupervised learning[C]//Signals, Systems and Computers (ASILOMAR), 2012 Conference Record of the Forty Sixth Asilomar Conference on. IEEE, 2012: 386-390.

[19] Jiang H, Zhang J J, Gao D W, et al. Synchrophasor based auxiliary controller to enhance power system transient voltage stability in a high penetration renewable energy scenario[C]//Power Electronics and Machines for Wind and Water Applications (PEMWA), 2014 IEEE Symposium. IEEE, 2014: 1-7.

[20] Jiang H, Zhang Y, Zhang J J, et al. Synchrophasor-based auxiliary controller to enhance the voltage stability of a distribution system with high renewable energy penetration[J]. IEEE Transactions on Smart Grid, 2015, 6(4): 2107-2115.

[21] Alejandro J, Arce A, Bordons C. Hybrid model predictive control of a two-generator power plant integrating photovoltaic panels and a fuel cell[C]//Decision and Control, 2007 46th IEEE Conference on. IEEE, 2007: 5447-5452.

[22] Minchala-Avila L I, Vargas-Martínez A, Zhang Y, et al. A model predictive control approach for integrating a master generation unit in a microgrid[C]//2013 Conference on Control and Fault-Tolerant Systems (SysTol). IEEE, 2013: 674-679.